CHARACTERISTICS OF NANOPARTICLE EMISSIONS FROM AN AGED DIESEL VEHICLE FUELLED WITH BIODIESEL B7

Tanakorn Uthaiphetra[1], Ekarong Sukjit[2], Pirutchada Musigapong[1], Kewalee Prompiputtanapon[3] and Kiattisak Batsungnoen[1,*]

Received: February 17, 2026; Revised: April 27, 2026; Accepted: May 12, 2026

Abstract

Emissions from aging diesel vehicles represent a major environmental and public health concern, particularly in view of the widespread use of biodiesel blends in existing fleets. This study investigates the nanoparticle emissions from an aged diesel passenger vehicle fuelled with biodiesel B7 under simulated driving conditions. The numbers and mass concentrations of the particles and their size distributions, morphology, and elemental composition are recorded at engine start-up, while driving at low (50 km/h) and high speeds (100 km/h), and after driving, using a chassis dynamometer and multiple measurement techniques. The particulate emissions are found to be dominated by ultrafine particles (<100 nm). The number concentrations vary between 1.35×10^7 particles/cm³ during engine start-up and 2.60×10^7 particles/cm³ during high-speed driving, with concentrations inside the exhaust pipe approximately 7.8 times higher than those measured outside. Morphological analysis reveals a transition from compact agglomerates under low-speed conditions to fractal-like, porous aggregates at high speed. Higher proportions of iron (Fe) and sulphur (S) are found during high-speed driving, suggesting influences from engine wear and lubricant-related sources. The small sizes and high reactivity of these particles allow them to penetrate into the lungs and enter the bloodstream, posing respiratory and cardiovascular health risks. Characterisation based on particle numbers and physicochemical properties is therefore preferable to mass-based emission metrics in terms of capturing the health-related features of diesel exhaust. Ultrafine particle exposure should be prioritised in environmental and occupational health risk assessments, particularly in regions with a high proportion of aging diesel vehicles.

Keywords: **Biodiesel B7; Diesel exhaust emissions; Ultrafine particles; Nanoparticles; Particle morphology; Occupational health risk**

---

[1] *Institute of Public Health, Suranaree University of Technology, Nakhon Ratchasima 30000, Thailand, E-mail: Tanakorn312525@gmail.com, ORCID: 0009-0005-4555-5821; pirutchada@sut.ac.th, ORCID: 0000-0001-9125-2139; kiattisak@sut.ac.th, ORCID: 0000-0003-4957-6548*

[2] *School of Mechanical Engineering, Institute of Engineering, Suranaree University of Technology, Nakhon Ratchasima 30000, Thailand. E-mail: ekarong@sut.ac.th, ORCID: 0000-0003-4641-2580*

[3] *Center for Scientific and Technological Equipment, Suranaree University of Technology, Nakhon Ratchasima 30000, Thailand, E-mail: kewalee@sut.ac.th, ORCID: 0000-0001-9125-2139*

[*] *Corresponding author*

DOI: https://doi.org/10.55766/sujst13042

Suranaree J. Sci. Technol. 33(5):070118(1-12)

Introduction

Increasing levels of air pollution, and particularly particulate matter, remain a significant environmental issue, especially in urban areas where traffic congestion is prevalent. One major contributor to air pollution is the presence of diesel vehicles, as these emit ultrafine particles, also referred to as nanoparticles, which can penetrate deep into the human respiratory system and cause long-term adverse health effects (Sydbom *et al.*, 2001; Oberdörster *et al.*, 2005). In developing countries such as Thailand, a substantial proportion of the diesel vehicles form part of aging fleets, often with more than 10 years of service and without advanced emission control technologies. These vehicles tend to emit significantly higher levels of particulate matter than newer models, making them an important target for emissions testing (Caliskan & Mori, 2017); however, data on their emissions remain limited, particularly under real-world conditions and when fuelled with biodiesel (Tunno *et al.*, 2016; Taxell & Santonen, 2017).

Biodiesel B7 is a blended fuel consisting of 7% fatty acid methyl esters (FAMEs) and 93% conventional petroleum diesel. It is widely used, due to its compatibility with existing diesel engines and fuel infrastructure (Boichenko *et al.*, 2025). The adoption of B7 has been promoted as a strategy to reduce dependence on fossil fuels and mitigate environmental impacts, for example by lowering carbon dioxide emissions (de Oliveira *et al.*, 2015). In addition, B7 provides economic benefits, particularly in Thailand, where the cultivation of palm oil supports the domestic production of biodiesel, thereby reducing reliance on imported fossil fuels in accordance with government policies promoting renewable energy. From a lifecycle perspective, the use of renewable feedstocks such as palm oil can reduce the overall carbon footprint at the fuel production and usage stages, contributing to a more sustainable energy system. Compared with conventional diesel (B0), B7 has been reported to yield particle number concentrations that are reduced by more than 10%, and to emit lower levels of black carbon under various engine operating conditions (Ajtai *et al.*, 2024). Despite these advantages, however, B7 is also subject to certain limitations; for example, although it can reduce overall carbon emissions, studies have shown that it may lead to increased emissions of fine particles under specific operating conditions (Prakash *et al.*, 2022). Diesel exhaust nanoparticles contribute to ambient PM 2.5 levels, degrade air quality, participate in atmospheric processes, and transport toxic substances such as metals, with potential effects on environmental systems (Rönkkö *et al.*, 2023). Furthermore, the use of biodiesel may not fully eliminate other harmful pollutants, and in older diesel engines can result in elevated particulate emissions, including nanoparticles that pose significant health risks (Reşitoğlu *et al.*, 2015; Aljaafari *et al.*, 2022). Nanoparticles are mainly formed from incomplete combustion in diesel engines, which causes the formation of soot precursors and ultrafine particles (Lapuerta *et al.*, 2008). The oxygen content of the FAMEs in B7 alters the combustion and the formation of soot, and under certain conditions may enhance nucleation and increase the formation of ultrafine particles, especially in aged engines (Chien *et al.*, 2009).

The nanoparticles emitted from aged diesel vehicles operating on biodiesel B7 are of particular concern due to their extremely small size (less than 100 nm) and high surface reactivity. These particles can bypass the body's natural respiratory defence mechanisms and penetrate deeply into the lungs, where they may enter the bloodstream. Exposure to such particles has been associated with systemic inflammation, oxidative stress, and cellular damage, all of which increase the risk of respiratory disease, including chronic obstructive pulmonary disease, asthma, and lung cancer (Kumar *et al.*, 2013; Portugal *et al.*, 2024). Exposure to ultrafine particles has also been linked to cardiovascular disease, as these particles can influence blood pressure, increase arterial stiffness, and promote atherosclerosis (Rabe *et al.*, 2007). Consequently, emissions of fine and ultrafine particles from older diesel engines fuelled with B7 give rise to both public health risks and environmental pollution, underscoring the need for comprehensive studies in order to fully understand their impacts (Mehus *et al.*, 2015).

Despite growing global concern over the environmental and health impacts of diesel emissions, and especially nanoparticle emissions, data on particulate emissions from aged diesel vehicles operating on biodiesel B7 remain limited. This knowledge gap highlights the need for further research into the characteristics of nanoparticle emissions from these vehicles. Relatively few authors have conducted simultaneous examinations of the number and mass concentrations of particles, their size distributions and morphology, and the elemental composition of emissions from aged diesel engines fuelled with biodiesel B7 under simulated driving conditions. The aim of this study is therefore to investigate the nanoparticle emissions from aged diesel engines fuelled with

biodiesel B7 under various simulated driving conditions in a controlled environmental setting. Through careful characterisation of the elemental composition, size distribution, and morphology of the particles, this research provides valuable insights into the potential health risks associated with long-term exposure, particularly with respect to respiratory and cardiovascular outcomes. The findings are expected to support improved public health monitoring, inform regulatory development, and contribute to mitigation strategies for diesel-related emissions under simulated driving conditions.

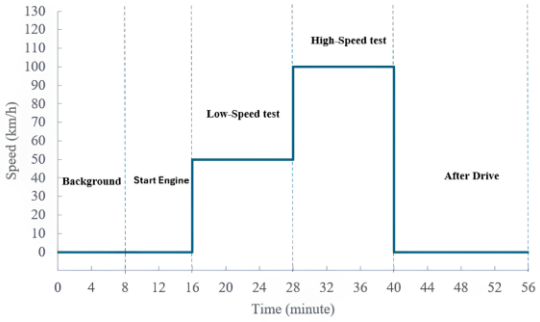


Figure 1. Schematic overview of the experimental sequence for particle emission measurements during the combustion of biodiesel B7

Materials and Methods

The focus of this study is on the number size distribution, number concentration, mass distribution and morphology of the particles and their elemental composition under simulated driving conditions at different vehicle speeds. The findings are expected to provide experimental evidence that can support environmental and occupational exposure assessments and contribute to informed evaluations of biodiesel fuel use in existing diesel vehicle fleets. A four-stroke diesel passenger vehicle with a service life exceeding 10 years, equipped with a 2,500 cc engine and a maximum torque of 329 Nm at 1,800 rpm, and fuelled with biodiesel B7, was tested using a chassis dynamometer (FPS 2700). The test vehicle had an accumulated mileage of approximately 156,290 km. The vehicle was manufactured under the Euro 3 emissions standard, which did not require the installation of advanced particulate emission control technologies. Hence, the exhaust system of the tested diesel vehicle was not equipped with a diesel particulate filter or an exhaust gas recirculation system.

Experimental Procedure

The experimental procedure was adapted from the approach reported by (Chaiyakham *et al.*, 2024), and consisted of five sequential steps. In Step 1, background particle concentrations were measured over 8 min under baseline conditions. In Step 2, the engine was started and allowed to operate at idle for 8 min. In Step 3, the vehicle was driven at a constant speed of 50 km/h for 12 min, and Step 4, the vehicle speed was increased to 100 km/h and maintained for 12 min. Upon completion of the driving phases, the engine was switched off, during which post-driving particle concentrations were monitored in Step 5 for 16 min. All experiments were performed in triplicate, as illustrated in Figure 1.

Measurements of the Number and Mass Distributions and Concentrations

Internal Exhaust Measurements

To enable measurements within the pipe, the particle measurement head of an Engine Exhaust Particle Sizer (EEPS™) spectrometer (TSI Model 3090, TSI Inc., Minnesota, USA) was installed directly inside the exhaust pipe. This instrument was used to measure the number and mass concentrations of the particles as a function of their size. Particle size distributions were recorded over the range 5.6-560 nm, with data collected at 1 s intervals. Measurements were conducted continuously based on Steps 1 to 4 of the experimental procedure, as illustrated in Figure 2.

External Exhaust Measurements

For the out-of-pipe measurements, a portable aerosol spectrometer (Dust Decoder 11-D, DURAG Group, Muldestausee, Germany) covering a particle size range of 250-35,000 nm was used together with a scanning mobility particle sizer coupled with a condensation particle counter (SMPS+C) (Model 5416, DURAG Group, Muldestausee, Germany), which measured particles in the range 10-1,090 nm. These two instruments were operated simultaneously and the results were integrated using Wide Range software to generate a combined particle size distribution spanning 10-35,000 nm. This integrated measurement system was used to determine both the number concentration and mass concentration of the particles measured outside the exhaust pipe. The sampling inlets were positioned at a height of 150 cm above the ground, corresponding to the approximate breathing zone of a standing adult, and at a horizontal distance of 100 cm from the exhaust outlet. This configuration was selected to give a realistic representation of the potential for inhalation exposure to vehicle

exhaust particles and to provide measurements that are directly relevant to environmental and occupational exposure assessments. Measurements were made continuously based on Steps 1 to 4 of the experimental procedure, as illustrated in Figure 2.

Elemental and Morphology Measurements

Elemental and morphological analyses were performed on particle samples collected outside the exhaust pipe under both low-speed and high-speed driving conditions. Nanoparticle sampling was conducted using a nanoparticle sampler that was equipped with 25 mm polycarbonate filter membranes with a pore size of 0.8 μm and connected to a calibrated air sampling pump (Universal PCXR8 Pump, KC Inc., Pittsburgh, USA). The sampling flow rate was maintained at 0.3 L min^{-1}. Samples were collected in Step 3 of the experimental procedure, corresponding to the first driving condition, with a sampling duration limited to 1 min to prevent filter overloading and excessive particle deposition. During sampling, the ambient relative humidity was maintained within the range 40-70% to minimise the influence of moisture on particle collection and analysis.

After sampling, the filter membranes were coated with gold to enhance their electrical conductivity prior to analysis. The samples were then analysed using field emission scanning electron microscopy combined with energy dispersive X-ray spectroscopy to characterise the particle morphology and determine the elemental composition. The experimental setup is illustrated in Figure 2.

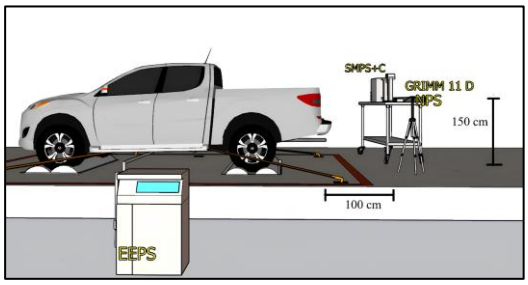


Figure 2. Schematic illustration of the experimental setup

Measured Fuel Properties of B7 Diesel

The properties of the fuel were found to be consistent with those of the B7 diesel fuel commonly used in Thailand. Following the notification issued by the Department of Energy Business on the specification and quality of diesel fuel, ASTM standard methods were used for analysis of the fuel properties, including ASTM D1298 for specific gravity, ASTM D613 for cetane number, ASTM D445 for kinematic viscosity, and ASTM D93 for flash point.

Results and Discussion

The physicochemical properties of the biodiesel B7 fuel used in this study were evaluated in accordance with the ASTM standards described above. The results confirmed that all of the measured parameters met the fuel quality requirements, indicating that the B7 fuel was suitable for diesel combustion in terms of ignition performance, fuel stability, and handling safety. The fuel had a flash point of 80°C, a cetane number of 58.37, a kinematic viscosity of 3.5 cSt, and a specific gravity of 0.845. These results are illustrated in Figure 3.

Particle Number Concentration and Size Distribution

Internal Exhaust Measurements

The particle number concentration measured inside the exhaust pipe was high under all engine operating conditions. As the engine was started, the concentration was 1.35 × 10^7 particles/cm^3, and increased slightly to 1.47 × 10^7 particles/cm^3 under low-speed driving conditions (50 km/h). The highest concentration was observed at high speed (100 km/h), with a value of 2.60 × 10^7 particles/cm^3. After the driving phase, the concentration decreased to 1.84 × 10^6 particles/cm^3. These results are illustrated in Figure 4(a).

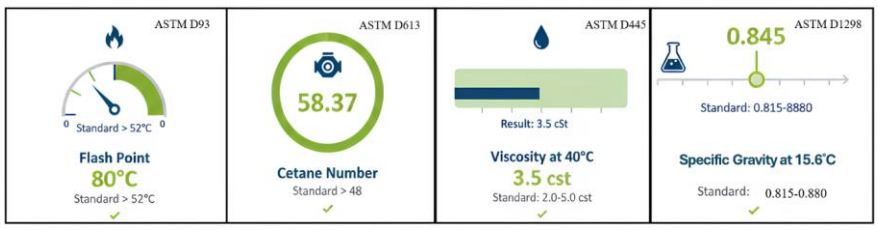


Figure 3. Physicochemical properties of the biodiesel B7 fuel evaluated based on ASTM standards

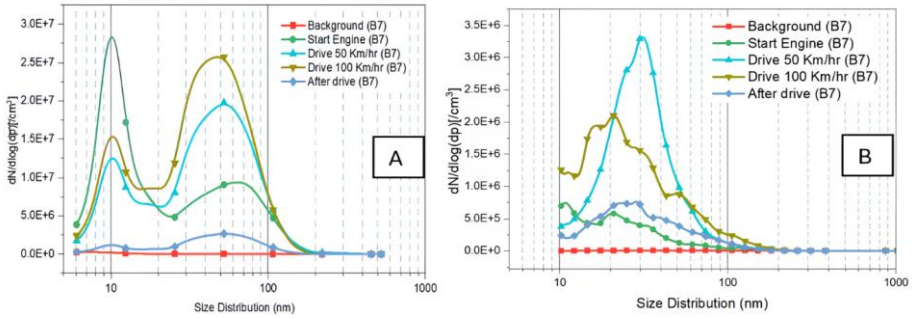


Figure 4. Particle size distributions and concentrations: (A) inside exhaust pipe; (B) outside exhaust pipe

External Exhaust Measurements

The particle number concentration measured outside the exhaust pipe was consistently lower than inside the exhaust pipe under all conditions. As the engine was started, the concentration was 3.47×10^5 particles/cm³, and this increased to 1.24×10^6 particles/cm³ under low-speed driving conditions (50 km/h). The highest concentration was observed at high speed (100 km/h), with a value of 3.33×10^6 particles/cm³, followed by a decrease to 4.50×10^5 particles/cm³ after driving. The results are illustrated in Figure 4(b).

A comparison between these internal and external measurements shows that the particle number concentrations inside the exhaust pipe were significantly higher under all operating conditions. The ratios were approximately 38.9 times higher during starting of the engine, 11.9 times higher under low-speed conditions (50 km/h), 7.8 times higher under high-speed conditions (100 km/h), and 4.1 times higher after driving. These results reflect the effects of dilution and particle transformation processes following emission from the exhaust source.

The differences observed between the particle number size distributions measured inside and outside the exhaust pipe may be attributed to several transformation processes that occur after the exhaust plume is released into the surrounding air. Immediately after emission, exhaust particles rapidly mix with the ambient air, leading to strong dilution of the exhaust plume and a substantial reduction in the particle number concentration (Harrison *et al.*, 2021). Aerosol dynamic processes such as particle coagulation and condensation of semi-volatile compounds during exhaust cooling can also significantly modify both the particle size distribution and particle number concentration. These processes promote the amalgamation of smaller particles into larger aggregates, resulting in a shift in the particle size distribution toward larger diameters and a decrease in particle number concentration. Furthermore, interactions with ambient particles and changes in temperature and humidity conditions may influence the particle transformation dynamics in the near-field environment. Similar transformation processes have also been reported in studies of the dynamics of diesel exhaust nanoparticles and plume evolution under atmospheric conditions (Louis *et al.*, 2017). Of these processes, dilution is likely to be the dominant factor under the present experimental conditions, due to the immediate mixing of exhaust emissions with surrounding air at the sampling location (D. Li *et al.*, 2024).

Nanoparticles are of particular concern for human health, because their extremely small size allows them to penetrate deeply into the alveolar region of the lungs and may enable translocation into the bloodstream (Raftis & Miller, 2019), affecting other organs. In addition, the particle number concentration is an important indicator for evaluating exposure to ultrafine particles, as nanoparticles occur in very large numbers (CCAC, 2016). Since they contribute only a small fraction of the particulate mass, the particle number concentration is considered to be a more appropriate metric for assessing nanoparticle exposure and potential health effects (Pope & Dockery, 2006).

Particle Mass Concentrations and Size Distributions

Internal Exhaust Measurements

The particle size distributions measured inside the exhaust pipe under all operating conditions (engine start, driving at 50 km/h, driving at 100 km/h, and after driving) were predominantly within the size range 25-200 nm. The particle mass concentrations were consistently high across all conditions, with values of 1.35×10^3 µg/m³ during engine start, 3.92×10^3 µg/m³ at 50 km/h and 4.15×10^3 µg/m³ (the highest value) at 100 km/h. After the driving phase, the concentration decreased to 2.74×10^2 µg/m³. These results are illustrated in Figure 5(a).

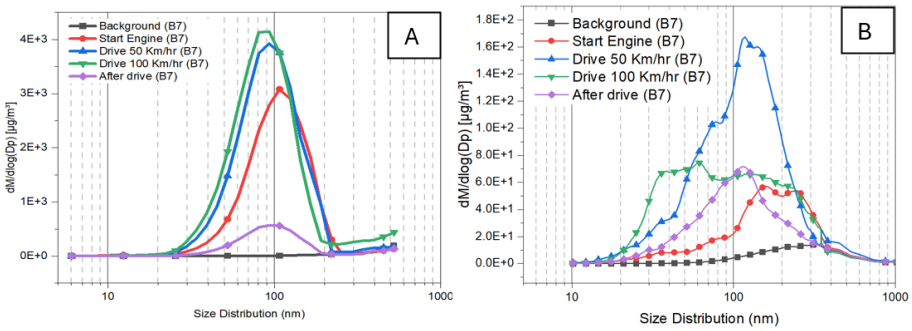


Figure 5. Particle mass size distribution and concentration: (A) inside the exhaust pipe; (B) outside the exhaust pipe

External Exhaust Measurements

The particle size distribution measured outside the exhaust pipe exhibited a broader range, extending approximately from 10 to 300 nm. The corresponding particle mass concentrations were substantially lower than those measured inside the exhaust pipe, with values of 4.78×10^1 µg/m³ during starting of the engine, 1.08×10^2 µg/m³ at 50 km/h, and 1.85×10^2 µg/m³ at 100 km/h. After driving, the concentration decreased to 9.31×10^1 µg/m³. These results are illustrated in Figure 5(b).

A comparison between the internal and external measurements shows that particle mass concentrations inside the exhaust pipe were consistently higher under all operating conditions. The differences were most pronounced during low-speed driving (36.3 times higher), followed by engine start (28.2 times higher) and high-speed driving (22.4 times higher), while a smaller difference was observed after driving (2.9 times higher). The broader particle size distribution observed outside the exhaust pipe suggests the influence of dilution and particle transformation processes following emission.

The observed differences in particle mass distribution between measurements conducted inside and outside the exhaust pipe can be attributed to processes that preferentially affect particle mass rather than particle number. After emission, larger particles contribute more significantly to the mass concentration and are more prone to gravitational settling and surface deposition, leading to a reduction in the measured mass at external sampling locations. In addition, dilution reduces the overall particle mass concentration, while particle transformation processes may alter the particle sizes through restructuring and growth. Taken together, these mechanisms result in a broader, shifted mass size distribution outside the exhaust pipe. Similar behaviour has been reported in studies of diesel exhaust particle dynamics and atmospheric transformation processes (Kittelson *et al.*, 2022; Zhang *et al.*, 2025a).

The observed differences in particle mass concentration across different vehicle speeds can be attributed to variations in the engine operating conditions, and particularly the engine load and combustion characteristics. At higher vehicle speeds (100 km/h), the engine operates under increased load and fuel consumption, which can lead to higher combustion temperatures and enhanced soot formation, resulting in elevated particle mass concentrations. In contrast, lower vehicle speeds (50 km/h) are generally associated with reduced engine load and more stable combustion conditions, leading to lower particulate mass emissions. The increased exhaust flow rates at higher speeds may also contribute to the transport and emission of particulate matter. Similar trends have been reported in studies of diesel engine emissions under varying operating conditions (Kittelson *et al.*, 2022).

Environmental and Occupational Exposure Parameters

Environmental Parameters

The mass concentrations classified by environmental parameters (TSP, PM10, PM2.5, and PM1) varied across the experimental conditions. These are widely used as indicators for air quality assessment (WHO, 2021). The highest mass concentration was observed for TSP under the 100 km/h driving condition, with a value of 32.73 µg/m³, representing an increase of approximately 1.93 times compared with background levels. Smaller particle fractions showed similar increasing trends, with maximum concentrations of 30.71 µg/m³ for PM10, 27.51 µg/m³ for PM4, 25.40 µg/m³ for PM2.5, and 22.88 µg/m³ for PM1.

As illustrated in Figure 6(A), higher mass concentrations were found for the engine starting

phase than for the 50 km/h driving condition. This can be attributed to the more incomplete combustion processes during engine start-up, whereas combustion becomes more efficient during steady state driving, resulting in lower particulate emissions. However, it should be noted that the driving tests were conducted under constant speed conditions, meaning that variations in engine speed and load were limited. This experimental constraint may have reduced the sensitivity of the measurements in terms of capturing differences in emissions associated with dynamic driving conditions (Zhang *et al.*, 2025b)

The observed distribution pattern for the particle mass concentration (TSP > PM10> PM4 > PM2.5 > PM1) arises from the hierarchical nature of size-segregated particulate matter, in which larger size fractions include the mass contributions of smaller particles (Damiati *et al.*, 2025). TSP represents the total range of airborne particles, while smaller fractions correspond to progressively lower aerodynamic cut-offs, resulting in lower mass concentrations (Suchánková *et al.*, 2024). Coarse particles also contribute more to the total mass due to their larger size, whereas fine and ultrafine particles contribute less despite their high number concentrations (Ćirović *et al.*, 2026).

Occupational Parameters

The mass concentrations classified by occupational parameter (inhalable, thoracic, and respirable dust) also showed variations across driving conditions. These were defined based on established airborne exposure conventions (ISO, 1995; Patel & Aggarwal, 2022). The highest mass concentration was observed for inhalable dust under the 100 km/h driving condition, corresponding to an increase of approximately 3.5 times relative to background levels. Similar increasing patterns were seen for all occupationally relevant particle size fractions, with maximum concentrations of 59.79 µg/m³ for inhalable dust, 51.03 µg/m³ for thoracic dust, and 46.18 µg/m³ for respirable dust.

As shown in Figure 6(B), inhalable dust consists of particles that are capable of entering the upper respiratory tract, whereas thoracic dust can penetrate into the lower airways, and respirable dust can reach the alveolar region and potentially enter the bloodstream, thereby posing greater health risks (Moazami *et al.*, 2023). These size-selective occupational exposures have been strongly associated with adverse respiratory outcomes and impaired pulmonary function in occupational settings (Vinnikov *et al.*, 2023). Moreover, evidence increasingly suggests that long-term exposure to occupational dust contributes to multisystem health effects, with both respiratory and cardiovascular impacts (M. Li *et al.*, 2025).

The hierarchy of occupational dust fractions (inhalable > thoracic > respirable) is governed by size-selective sampling and particle aerodynamic behaviour. Inhalable particles enter the respiratory system, whereas only the smaller fractions penetrate into the lower airways and alveolar region (Brown *et al.*, 2013; Wippich *et al.*, 2020). As the particle size decreases, the fraction of particles capable of deep lung deposition is reduced, resulting in progressively lower mass concentrations, as observed in occupational exposure measurements (Mastrantonio *et al.*, 2021).

An association between environmental and occupational mass concentrations arises from overlapping ranges of particle sizes. Fine particles (PM2.5 and PM1) are the respirable and thoracic fractions capable of penetrating the lower respiratory tract (Moazami *et al.*, 2023), while coarse particles (TSP and PM10) represent inhalable fractions that are deposited in the upper airways (Patel & Aggarwal, 2022), indicating that particle size governs both the environmental distribution and health-relevant deposition. Moreover, nanoparticles and particles smaller than PM1 can translocate from the alveolar region into the bloodstream to reach secondary organs, giving rise to systemic health risks (Qi *et al.*, 2023)

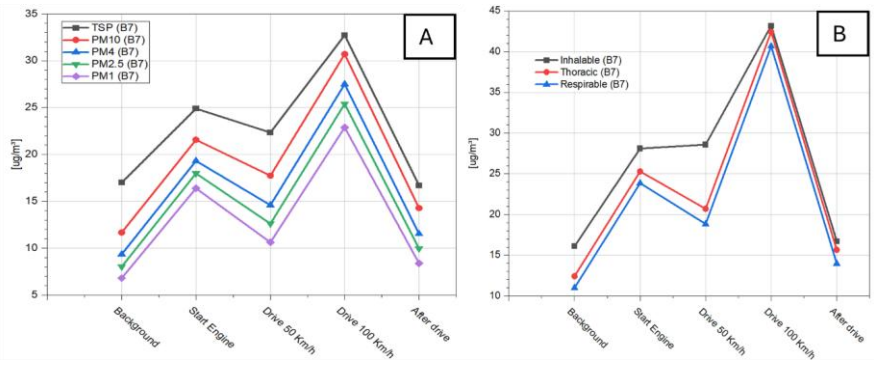


Figure 6. Particle mass concentrations classified by: (A) environmental parameters; (B) occupational parameters

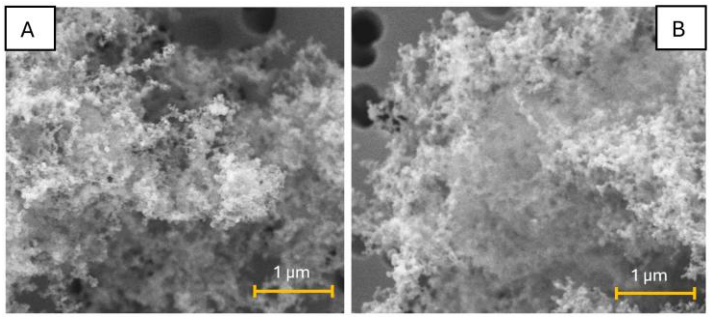


Figure 7. Photographs showing the morphology of exhaust particles at 10,000× magnification: (A) particles emitted at 50 km/h; (B) particles emitted at 100 km/h

Particle Morphology

Under low-speed driving conditions (50 km/h), particles predominantly formed large agglomerates with irregular shapes and rough surfaces. These agglomerates were compact and densely packed, consisting of multiple primary particles that coalesced under relatively mild combustion conditions and lower exhaust gas velocities. At lower engine loads, the combustion temperature and turbulence intensity are generally reduced, thus limiting soot nucleation while promoting the condensation of semi-volatile organic compounds on existing particle surfaces. These processes enhance the restructuring and compaction of particles, resulting in denser soot agglomerates with lower internal porosity (Li *et al.*, 2021; Wang *et al.*, 2024). This morphology also suggests longer particle residence times within the exhaust system, favouring particle–particle collisions and structural consolidation. Representative particle morphologies observed under low-speed driving conditions are shown in Figure 7(a) (Neer & Koylu, 2006; Liu *et al.*, 2021).

In contrast, particles generated under high-speed driving conditions (100 km/h) formed more open, complex and fractal-like aggregate structures composed of smaller primary particles. These aggregates appeared highly porous and less compact compared with those formed under low-speed conditions. High-speed driving typically involves higher engine loads and elevated combustion temperatures, which enhance the formation of soot precursors, particle nucleation, and surface growth. The increase in the velocity and turbulence intensity of the exhaust gas can significantly increase the particle-particle collision frequency within the exhaust flow (Arora *et al.*, 2023). Under such conditions, soot particles tend to aggregate via diffusion-limited aggregation processes, forming open chain-like or fractal structures composed of numerous primary nanoparticles (Guarieiro *et al.*, 2017; Baldelli *et al.*, 2020). The intensified flow dynamics and reduced residence time inhibit the formation of compact agglomerates, resulting in loosely bound particles with higher specific surface area. Typical examples of particle structures observed under high-speed driving conditions are shown in Figure 7(b). (China *et al.*, 2014).

From a toxicological perspective, fractal and highly porous particles have a larger effective surface area and higher chemical reactivity than compact agglomerates, which enhances their ability to induce oxidative stress and inflammatory responses following inhalation. The predominance of fractal-like structures under high-speed driving conditions therefore indicates a higher toxicological burden arising from particles emitted from aged diesel engines fuelled with biodiesel B7, even when the overall particle mass concentration is not significantly elevated (Du *et al.*, 2022).

Elemental Composition Analysis

The elemental composition of particulate matter emitted due to biodiesel B7 combustion in an aged diesel engine was analysed under low-speed (50 km/h) and high-speed (100 km/h) driving conditions. At the lower speed, higher relative abundances of carbon (C) and oxygen (O) were observed, suggesting incomplete combustion and enhanced condensation of organic compounds. The presence of silicon (Si) and chlorine (Cl) may also be associated with resuspended road dust, lubricant additives, or fuel impurities (China *et al.*, 2014). Compared with high-speed driving, the relative abundances of C, O, Si, and Cl under low-speed conditions were increased by factors of approximately 1.33, 1.33, 1.02, and 1.29, respectively.

In contrast, the particles emitted under high-speed driving conditions contained higher concentrations of magnesium (Mg), sulphur (S), and iron (Fe), indicating increased contributions from lubricant-derived components, fuel sulphur

content, and engine wear processes (Du *et al.*, 2022). The elevated Fe content suggests mechanical abrasion of the engine components, while the increased sulphur may promote the formation of sulphate particles during exhaust cooling. The relative abundances of Mg, S, and Fe at 100 km/h were approximately 2.71, 1.34, and 2.18 times higher, respectively, compared with those measured at 50 km/h.

The presence of metal-containing particles, particularly iron, is of concern due to their ability to catalyse redox reactions and enhance the reactivity of the particles, contributing to adverse biological effects following inhalation (Lelieveld *et al.*, 2020). Overall, these results demonstrate that driving conditions strongly influence the elemental composition of diesel exhaust particles, and that toxicological effects may increase at high speeds due to the elevated content of metal and sulphur. The results for the elemental composition are presented in Figure 8.

The source pathway receptor framework suggests that for effective mitigation of nanoparticle emissions, control at the source should be prioritised, followed by pathway interruption and receptor protection. Source control can be achieved by improving engine conditions, minimising engine wear, adopting advanced emission control technologies such as diesel particulate filters, and promoting cleaner fuels (Johnson, 2009). Pathway control involves reducing particle dispersion and exposure in the surrounding environment through improved ventilation, local exhaust systems, and maintaining adequate distance from emission sources (Morawska *et al.*, 2020), whereas receptor protection focuses on minimising human exposure, particularly in high-risk environments, through the use of high-efficiency respiratory protective equipment (e.g., P100 or FFP3 respirators) and implementing appropriate occupational safety measures (Cherrie *et al.*, 2018).

Limitations

This study has several limitations that should be acknowledged. The experiments were conducted using a single diesel vehicle, which may limit the generalisability of the results to other vehicle types or engine conditions. In addition, the experiments were conducted under simulated driving conditions in a controlled environment, which enabled precise control of vehicle speed and operating conditions and allowed for consistent and reproducible emission measurements.

Conclusions

In this study, particulate emissions from an aged diesel vehicle operating on biodiesel B7 were evaluated, with a focus on the particle number and mass concentrations, size distributions, morphology, and elemental composition under different driving conditions. Although the fuel complied with ASTM quality standards, substantial emissions of ultrafine and nanoparticle sized particles were observed, particularly during active driving and at higher vehicle speeds.

At the higher speed (100 km/h), the particle number concentrations were significantly higher than at the lower speed and the background conditions, both inside and outside the exhaust pipe. Emissions were dominated by nanoparticles, highlighting the limitations of mass-based metrics for assessing the health relevance of diesel exhaust. Particle mass concentrations were also influenced by driving conditions, with higher levels of the respirable and thoracic size fractions observed during high-speed operation. Morphological and elemental analyses indicated a shift toward fractal-like, porous aggregates and increased numbers of metal - and sulphur - containing particles at higher speeds, suggesting enhanced toxicological relevance.

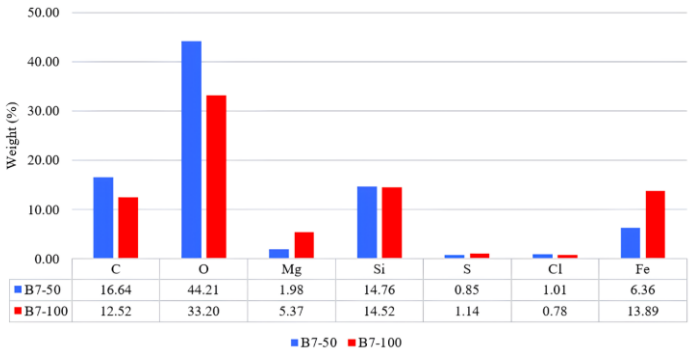


Figure 8. Elemental composition of particles emitted from an engine running on biodiesel B7 under low-speed (50 km/h) and high-speed (100 km/h) driving conditions

From the perspective of environmental and occupational health, these findings raise concerns due to the increased potential of ultrafine and metal-containing particles to induce oxidative stress and inflammatory responses following inhalation. Since the characteristics of the particles vary strongly with the driving conditions, risk reduction should follow an approach based on a hierarchy of controls. Engineering and administrative controls should be prioritised, and personal protective equipment may be required where higher-level controls are insufficient. In exposure scenarios dominated by nanoparticles, respiratory protection exceeding N95 or FFP2 standards (or equivalent certified devices) is recommended. The integration of these measures with monitoring based on particle numbers represents an approach that prioritises health when managing the risks associated with emissions from aging diesel vehicle fleets.

Funding

The authors received no specific financial support for the research, authorship, and/or publication of this article.

Author Contributions

Conceptualization: T.U., E.S., P.M., K.B.; Methodology: T.U., E.S., P.M., K.B.; Investigation: T.U., E.S., P.M., K.P., K.B.; Data Curation: T.U., E.S., P.M., K.B.; Writing - Original Draft: T.U., K.B.; Writing - Review & Editing: T.U., E.S., P.M., K.B.; Supervision: E.S., P.M., K.P., K.B. All authors have read and agreed to the published version of the manuscript.

Ethics Statement

Ethical approval for this study was granted through an exemption, under approval number EC-67-180 by The Human Research Ethics Committee of Suranaree University of Technology (HREC-SUT). This study was conducted as part of the thesis entitled “Exposure Assessment of Particles from Combustion in Diesel Engines Over 10 Years Old Under Various Biodiesel Fuel Conditions.

Declaration of Generative AI Use

The authors declare that no Generative AI tools were used in the preparation of this manuscript.

Conflict of Interest

The authors declare that they have no conflicts of interest related to this work.

Data Availability Statement

The datasets generated and/or analyzed during the current study are available in the Kiattisak Batsungnoen repository at kiattisak@sut.ac.th, ORCID: 0000-0003-4957-6548

Acknowledgement

This study was supported by Suranaree University of Technology (SUT).

References

Ajtai, T., Utry, N., Pintér, M., Rahman, A., Kurilla, B., Sárossy, G., Deák, L., Baladincz, J., Raffai, P., Szabó, G., & Bozóki, Z. (2024). The investigation of diesel soot emission using instrument combination of multi-wavelength photoacoustic spectroscopy and scanning mobility particle sizer. *Scientific Reports, 14*(1), Article 2254. https://doi.org/10.1038/s41598-024-52832-8

Aljaafari, A., Fattah, I. M. R., Jahirul, M. I., Gu, Y., Mahlia, T. M. I., Islam, M. A., & Islam, M. S. (2022). Biodiesel emissions: A state-of-the-art review on health and environmental impacts. *Energies, 15*(18), Article 6854. https://doi.org/10.3390/en15186854

Arora, P., Verma, P., Zare, A., Lodi, F., Jafari, M., Stevanovic, S., Bodisco, T. A., Brown, R. J., & Ristovski, Z. (2023). Morphology and nanostructure of soot particles from diesel engine under transient and steady-state operating conditions with a microalgae fuel component, dioctyl phthalate biofuel. *Sustainable Energy Technologies and Assessments, 60*, Article 103504. https://doi.org/10.1016/j.seta.2023.103504

Baldelli, A., Trivanovic, U., Corbin, J. C., Lobo, P., Gagné, S., Miller, J. W., Kirchen, P., & Rogak, S. (2020). Typical and atypical morphology of non-volatile particles from a diesel and natural gas marine engine. *Aerosol and Air Quality Research, 20*(4), 730-740. https://doi.org/10.4209/aaqr.2020.01.0006

Boichenko, S., Yakovlieva, A., Zubenko, S., & Shkilniuk, I. (2025). Physical, chemical, and performance properties of biodiesel fuels: A comparative study of lipid-based feedstocks. *Energies, 18*(16), Article 4274. https://doi.org/10.3390/en18164274

Brown, J. S., Gordon, T., Price, O., & Asgharian, B. (2013). Thoracic and respirable particle definitions for human health risk assessment. *Particle and Fibre Toxicology, 10*(1), Article 12. https://doi.org/10.1186/1743-8977-10-12

Caliskan, H., & Mori, K. (2017). Thermodynamic, environmental and economic effects of diesel and biodiesel fuels on exhaust emissions and nano-particles of a diesel engine. *Transportation Research Part D: Transport and Environment, 56*, 203-221. https://doi.org/10.1016/j.trd.2017.08.009

Chaiyakham, N., Boonruksa, P., Prompiputtanapon, K., & Batsungnoen, K. (2024). Characteristics of particulate matter emissions from a ten-year-old diesel pickup truck in laboratory driving simulations. *Journal of Medicine and Public Health, Ubon Ratchathani University, 7*(2), 117-128.

Cherrie, J. W., Apsley, A., Cowie, H., Steinle, S., Mueller, W., Lin, C., Horwell, C. J., Sleeuwenhoek, A., & Loh, M. (2018). Effectiveness of face masks used to protect Beijing residents against particulate air pollution. *Occupational and Environmental Medicine, 75*(6), 446-452. https://doi.org/10.1136/oemed-2017-104765

Chien, S.-M., Huang, Y.-J., Chuang, S.-C., & Yang, H.-H. (2009). Effects of biodiesel blending on particulate and polycyclic aromatic hydrocarbon emissions in nano/ultrafine/fine/coarse ranges from diesel engine. *Aerosol and Air Quality Research, 9*(1), 18-31. https://doi.org/10.4209/aaqr.2008.09.0040

China, S., Salvadori, N., & Mazzoleni, C. (2014). Effect of traffic and driving characteristics on morphology of atmospheric soot particles at freeway on-ramps. *Environmental Science & Technology, 48*(6), 3128-3135. https://doi.org/10.1021/es405178n

Ćirović, Ž., Stojanović, D. B., Davidović, M., Onjia, A., Alastuey, A., & Jovašević-Stojanović, M. (2026). New particle formation and source apportionment of particle number size distribution in the urban area of the city of Belgrade. *Atmosphere, 17*(2), Article 205. https://doi.org/10.3390/atmos17020205

Climate & Clean Air Coalition (CCAC). (2016). *Ambient air pollution: A global assessment of exposure and burden of disease*. https://www.ccacoalition.org/resources/ambient-air-pollution-global-assessment-exposure-and-burden-disease

Damiati, S., AlMashrea, B. A., Rabiei, N., Sujatha, A. P., Sabir, D. K., Alhosani, M., & Kodzius, R. (2025). Aerosol pollutants and health: Role of size and chemical composition. *Public Health Challenges, 4*(4), Article e70134. https://doi.org/10.1002/puh2.70134

de Oliveira, A., de Morais, A. M., Valente, O. S., & Sodré, J. R. (2015). Combustion characteristics, performance and emissions from a diesel power generator fuelled by B7-ethanol blends. *Fuel Processing Technology, 139*, 67-72. https://doi.org/10.1016/j.fuproc.2015.08.010

Du, J., Su, L., Zhang, D., Jia, C., & Yuan, Y. (2022). Experimental investigation into the pore structure and oxidation activity of biodiesel soot. *Fuel, 310*, Article 122316. https://doi.org/10.1016/j.fuel.2021.122316

Guarieiro, A. L. N., Eiguren-Fernandez, A., Rocha, G. O. da, & Andrade, J. B. de. (2017). An investigation on morphology and fractal dimension of diesel and diesel-biodiesel soot agglomerates. *Journal of the Brazilian Chemical Society, 28*(8), 1351-1362. https://doi.org/10.21577/0103-5053.20160306

Harrison, R., Allan, J. D., Heal, M. R., Lewis, A. C., Marner, B., Murrells, T., & Williams, A. (2021). Non-exhaust vehicle emissions of particulate matter and VOC from road traffic: A review. *Atmospheric Environment, 262*, Article 118592. https://doi.org/10.1016/j.atmosenv.2021.118592

International Organization for Standardization (ISO). (1995). *Air quality - Particle size fraction definitions for health-related sampling* (ISO 7708:1995). https://www.iso.org/standard/14534.html

Johnson, T. V. (2009). Review of diesel emissions and control. *International Journal of Engine Research, 10*(5), 275-285. https://doi.org/10.1243/14680874JER04009

Kittelson, D., Khalek, I., McDonald, J., Stevens, J., & Giannelli, R. (2022). Particle emissions from mobile sources: Discussion of ultrafine particle emissions and definition. *Journal of Aerosol Science, 159*, Article 105881. https://doi.org/10.1016/j.jaerosci.2021.105881

Kumar, S., Verma, M. K., & Srivastava, A. K. (2013). Ultrafine particles in urban ambient air and their health perspectives. *Reviews on Environmental Health, 28*(2-3), 117-128. https://doi.org/10.1515/reveh-2013-0008

Lapuerta, M., Armas, O., & Rodríguez-Fernández, J. (2008). Effect of biodiesel fuels on diesel engine emissions. *Progress in Energy and Combustion Science, 34*(2), 198-223. https://doi.org/10.1016/j.pecs.2007.07.001

Lelieveld, J., Pozzer, A., Pöschl, U., Fnais, M., Haines, A., & Münzel, T. (2020). Loss of life expectancy from air pollution compared to other risk factors: A worldwide perspective. *Cardiovascular Research, 116*(11), 1910-1917. https://doi.org/10.1093/cvr/cvaa025

Li, D., Wu, D., Gui, X., Liao, S., Zhu, M., Yu, F., & Zheng, J. (2024). Exploring ultrafine particle emission characteristics from in-use light-duty diesel trucks in China using a portable measurement system. *Environmental Research, 263*, Article 120234. https://doi.org/10.1016/j.envres.2024.120234

Li, M., Wu, C., Zhang, Y., Jiang, Y., Lin, J., & Xiang, J. (2025). Effects of occupational dust exposure on the health status of workers in China. *Scientific Reports, 15*(1), Article 19487. https://doi.org/10.1038/s41598-025-04014-3

Li, R., Wang, Z., Tang, C., & Meng, X. (2021). Study on particulate structure characteristics of diesel engines fueled with a methanol/biodiesel blend. *ACS Omega, 6*(9), 6081–6087. https://doi.org/10.1021/acsomega.0c04371

Liu, H., Yu, Y., Wang, C., Xu, H., & Ma, X. (2021). Brownian coagulation of particles in the gasoline engine exhaust system: Experimental measurement and Monte Carlo simulation. *Fuel, 303*, Article 121340. https://doi.org/10.1016/j.fuel.2021.121340

Louis, C., Liu, Y., Martinet, S., D'Anna, B., Valiente, A. M., Boreave, A., R'Mili, B., Tassel, P., Perret, P., & André, M. (2017). Dilution effects on ultrafine particle emissions from Euro 5 and Euro 6 diesel and gasoline vehicles. *Atmospheric Environment, 169*, 80-88. https://doi.org/10.1016/j.atmosenv.2017.09.007

Mastrantonio, R., Civisca, A., Siciliano, E., Inglese, E., Lippolis, T., Pompei, D., Cococcetta, L., Scatigna, M., & Fabiani, L. (2021). Exposure assessment to inhalable and respirable dust in the post-earthquake construction sites in the city of l'Aquila. *Journal of Occupational Health, 63*(1), Article e12296. https://doi.org/10.1002/1348-9585.12296

Mehus, A. A., Reed, R. J., Lee, V. S. T., Littau, S. R., Hu, C., Lutz, E. A., & Burgess, J. L. (2015). Comparison of acute health effects from exposures to diesel and biodiesel fuel emissions. *Journal of Occupational and Environmental Medicine, 57*(7), 705-712. https://doi.org/10.1097/JOM.0000000000000473

Moazami, T. N., Svendsen, K. v. H., Buhagen, M., & Jørgensen, R. B. (2023). Comparing PM2.5, respirable dust, and total dust fractions using real-time and gravimetric samples in an exposure chamber study. *Heliyon, 9*(6), Article e16127. https://doi.org/10.1016/j.heliyon.2023.e16127

Morawska, L., Tang, J. W., Bahnfleth, W., Bluyssen, P. M., Boerstra, A., Buonanno, G., Cao, J., Dancer, S., Floto, A., Franchimon, F., Haworth, C., Hogeling, J., Isaxon, C., Jimenez, J. L., Kurnitski, J., Li, Y., Loomans, M., Marks, G., Marr, L. C., … Yao, M. (2020). How can airborne transmission of COVID-19 indoors be minimised? *Environment International, 142*, Article 105832. https://doi.org/10.1016/j.envint.2020.105832

Neer, A., & Koylu, U. O. (2006). Effect of operating conditions on the size, morphology, and concentration of submicrometer particulates emitted from a diesel engine. *Combustion and Flame, 146*(1), 142–154. https://doi.org/10.1016/j.combustflame.2006.04.003

Oberdörster, G., Oberdörster, E., & Oberdörster, J. (2005). Nanotoxicology: An emerging discipline evolving

from studies of ultrafine particles. *Environmental Health Perspectives, 113*(7), 823-839. https://doi.org/10.1289/ehp.7339

Patel, P., & Aggarwal, S. G. (2022). On the techniques and standards of particulate matter sampling. *Journal of the Air & Waste Management Association, 72*(8), 791-814. https://doi.org/10.1080/10962247.2022.2048129

Pope, C. A., & Dockery, D. W. (2006). Health effects of fine particulate air pollution: Lines that connect. *Journal of the Air & Waste Management Association, 56*(6), 709-742. https://doi.org/10.1080/10473289.2006.10464485

Portugal, J., Bedia, C., Amato, F., Juárez-Facio, A. T., Stamatiou, R., Lazou, A., Campiglio, C. E., Elihn, K., & Piña, B. (2024). Toxicity of airborne nanoparticles: Facts and challenges. *Environment International, 190*, Article 108889. https://doi.org/10.1016/j.envint.2024.108889

Prakash, S., Prabhahar, M., & Saravana Kumar, M. (2022). Experimental analysis of diesel engine behaviours using biodiesel with different exhaust gas recirculation rates. *International Journal of Ambient Energy, 43*(1), 1508-1517. https://doi.org/10.1080/01430750.2020.1712251

Qi, Y., Chen, Y., Xia, T., Lynch, I., & Liu, S. (2023). Extra-pulmonary translocation of exogenous ambient nanoparticles in the human body. *ACS Nano, 17*(1), 12-19. https://doi.org/10.1021/acsnano.2c09299

Rabe, K. F., Hurd, S., Anzueto, A., Barnes, P. J., Buist, S. A., Calverley, P., Fukuchi, Y., Jenkins, C., Rodriguez-Roisin, R., van Weel, C., Zielinski, J., & Global Initiative for Chronic Obstructive Lung Disease. (2007). Global strategy for the diagnosis, management, and prevention of chronic obstructive pulmonary disease: GOLD executive summary. *American Journal of Respiratory and Critical Care Medicine, 176*(6), 532-555. https://doi.org/10.1164/rccm.200703-456SO

Raftis, J. B., & Miller, M. R. (2019). Nanoparticle translocation and multi-organ toxicity: A particularly small problem. *Nano Today, 26*, 8-12. https://doi.org/10.1016/j.nantod.2019.03.010

Reşitoğlu, İ. A., Altinişik, K., & Keskin, A. (2015). The pollutant emissions from diesel-engine vehicles and exhaust aftertreatment systems. *Clean Technologies and Environmental Policy, 17*(1), 15-27. https://doi.org/10.1007/s10098-014-0793-9

Rönkkö, T., Saarikoski, S., Kuittinen, N., Karjalainen, P., Keskinen, H., Järvinen, A., Mylläri, F., Aakko-Saksa, P., & Timonen, H. (2023). Review of black carbon emission factors from different anthropogenic sources. *Environmental Research Letters, 18*(3), Article 033004. https://doi.org/10.1088/1748-9326/acbb1b

Suchánková, L., Crumeyrolle, S., Bourrianne, E., Prokeš, R., Holoubek, I., & Chiapello, I. (2024). An insight into recent PM1 aerosol light scattering properties and particle number concentration variabilities at the suburban site ATOLL in Northern France. *Science of the Total Environment, 959*, Article 178190. https://doi.org/10.1016/j.scitotenv.2024.178190

Sydbom, A., Blomberg, A., Parnia, S., Stenfors, N., Sandström, T., & Dahlén, S.-E. (2001). Health effects of diesel exhaust emissions. *European Respiratory Journal, 17*(4), 733-746. https://doi.org/10.1183/09031936.01.17407330

Taxell, P., & Santonen, T. (2017). Diesel engine exhaust: Basis for occupational exposure limit value. *Toxicological Sciences, 158*(2), 243-251. https://doi.org/10.1093/toxsci/kfx110

Tunno, B. J., Dalton, R., Cambal, L., Holguin, F., Lioy, P., & Clougherty, J. E. (2016). Indoor source apportionment in urban communities near industrial sites. *Atmospheric Environment, 139*, 30-36. https://doi.org/10.1016/j.atmosenv.2016.04.039

Vinnikov, D., Romanova, Z., Raushanova, A., Beisbekova, A., Vitale, E., Bimuratova, G., & Rapisarda, V. (2023). Exposure to respirable particulate matter and its association with respiratory outcomes in beauty salon personnel. *International Journal of Environmental Research and Public Health, 20*(3), Article 2429. https://doi.org/10.3390/ijerph20032429

Wang, X., Wei, J., Zeng, Y., & Qian, Y. (2024). Diesel soot combustion in air-NO environment: Evolution of functional groups on soot surfaces. *Science of the Total Environment, 918*, Article 170579. https://doi.org/10.1016/j.scitotenv.2024.170579

Wippich, C., Rissler, J., Koppisch, D., & Breuer, D. (2020). Estimating respirable dust exposure from inhalable dust exposure. *Annals of Work Exposures and Health, 64*(4), 430-444. https://doi.org/10.1093/annweh/wxaa016

World Health Organization (WHO). (2021). *WHO global air quality guidelines: Particulate matter (PM2.5 and PM10), ozone, nitrogen dioxide, sulfur dioxide and carbon monoxide*. https://www.who.int/publications/i/item/9789240034228

Zhang, F., Peng, J., Zhang, J., Liu, J., Wu, Y., Liu, P., Liu, K., Sun, B., Zhang, Q., Wu, L., Yang, N., Hu, W., & Mao, H. (2025a). Real world particle size distribution from vehicle fleet and implication on emission control. *npj Clean Air, 1*(1), Article 8. https://doi.org/10.1038/s44407-025-00007-8

Zhang, J., Liu, G., & Xu, H. (2025b). Research on combustion and emissions of heavy duty diesel engines under low-speed and low-load conditions in low temperature environments. *PLOS ONE, 20*(2), Article e0318933. https://doi.org/10.1371/journal.pone.0318933